Proceeding of ICFDP 8:
Eighth International Congress of Fluid Dynamics & Propulsion
December 14-17, 2006, Sharm El-Shiekh, Sinai, Egypt.

ICFDP8–EG–166

FLOW AND HEAT TRANSFER CHARACTERISTICS AROUND A COMBINATION OF ELLIPTIC CYLINDERS IN-LINE

Aly A. Abdel Aziz[*], Nabil S. Berbish[*], and Abdalla, S. Hanafi[**]
***Mech. Eng. Dept. Shoubra Faculty of Eng. Benha Univ., Egypt.**
****Professor, Mech. Eng. Dept. Cairo University, Egypt**.

ABSTARCT

An experimental study has been conducted to investigate the heat transfer characteristics and flow behaviors around a single elliptic cylinder, and two elliptic cylinders in line. The cylinders having an axis ratio (b/c) 1:2, with zero angle of attack (major axis is horizontal) to the upstream uniform flow. Experiments were carried out for the downstream elliptic cylinder with uniform heat flux conditions, using air as the working fluid. The Reynolds number based on the upstream mean velocity and the major axis length, c, was ranged from about 3,450 to 45,420 and the longitudinal spacing ratio, (S_x/c), was varied from 1.5 to 4.0. It was found that, the average heat transfer coefficient for elliptic cylinder was higher than that for a circular cylinder. For two elliptic cylinders in-line arrangement, the heat transfer features and the flow characteristics around the downstream elliptic cylinder vary drastically with the cylinder spacing ratio (S_x/c). Also, the average Nusselt number for the downstream cylinder was higher by about 15-72 % than that of the single elliptic cylinder, depending on the cylinder spacing ratio. Moreover, a flow visualization study was made in order to show the flow features around the tested elliptic cylinders. Finally, the average Nusselt number was correlated in terms of the Reynolds number, and the cylinder spacing ratio.

KEYWORDS: Forced convection heat transfer, Flow behavior, Single elliptic cylinder, Two elliptic cylinders, In-line arrangement.

I. INTRODUCTION

Investigation of high-performance heat exchangers is an important and urgent problem for saving and making effective use of energy. Among many types of heat exchangers, those constructed of circular tubes have been used in many industries. Flow around the tubes, however, is not always normal to the tube axis. In such a situation, the cross section of the tube in the flow direction becomes an ellipse. An elliptic cylinder is a basic and general shape, which can become a flat plate in a special case and also a circular cylinder depending on its axis ratio. Furthermore, it is well known that its fluid dynamic drag at a small angle of attack is lower than that of a circular cylinder. This may be an advantageous feature when using elliptic tubes as a heat transfer surface element, since the pumping power required may be reduced and the heat exchanger may be more compact [1-3]. Relatively few theoretical and experimental studies have been carried out on flow and heat transfer from elliptic cylinders. Ota et al. [4] carried

out an experimental investigation to study heat transfer and flow around an elliptic cylinder of axis ratio 1:3. The angle of attack, α, is varied from zero to 90^o .It is found that the average heat transfer coefficient is at its highest at $\alpha=60^o - 90^o$ over the whole Reynolds number range studied, the lowest value of the average heat transfer rate is still higher than that for a circular cylinder. Ota and Nishiyama [5] studied experimentally the flow around two cylinders in-line arrangement. The elliptic cylinders examined had an axis ratio 1:3. It has been found that the flow characteristics vary drastically with the cylinder spacing ratio. Ota et al. [6] conducted experimentally forced convection heat transfer from two elliptic cylinders in-line arrangement, and their angles of attack to the upstream uniform flow are identical. It is found that the average Nusselt number shows great dependence upon the angle of attack and cylinder spacing ratio both for the upstream and downstream cylinders. Ota et al. [7] carried out an experimental investigation to study flow around an elliptic cylinder of axis ratio 1:3, in the critical Reynolds number ranged from 35,000 to 125,000. The results revealed that the critical Reynolds number depends on the angle of attack and attain a minimum value when the angle is between 5^o and 10^o. It was also found that a small separation bubble exists near the leading edge in the critical Reynolds number regime. Nishiyama et al. [8] performed an experimental investigation to clarify heat transfer characteristics and flow behaviors around four elliptic cylinders. They were placed in-line arrangement with a constant angle of attack to the upstream uniform flow. It has been found that the heat transfer features vary drastically with the angle of attack and also with the cylinder spacing ratio, corresponding to a great change in a flow features. Badr and Shamsher [9] studied theoretically free convection from an elliptic cylinder with major axis vertical. For a constant Rayleigh number, the average Nusselt number was found to increase with the decrease of the axis ratio approaching its maximum when the axis ratio approaches zero. Kondjoyan and Daudin [10] studied experimentally the effect of free stream turbulence intensity on heat and mass transfers at the surface of a circular cylinder and an elliptic cylinder of axis ratio 1:4. The influence of the elliptic cylinder ratio on the average transfer coefficients values was much less than the effect of the air flow properties. Also, it was found that the local heat transfer coefficient was much higher at the stagnation point of an elliptic cylinder than elsewhere at the surface. Chew et al. [11] studied theoretically the flow around an elliptic cylinder. It is found that, for zero angle of attack, the separation occurred later for slender elliptic cylinders. With increasing the aspect ratio, the separation points on both surfaces are moved upstream. Badr [12] conducted a theoretical study of laminar natural convection from an elliptic tube with different orientations. It is concluded that the maximum average Nusselt number is obtained when the tube major axis is vertical. Also, higher Rayleigh number leads to higher local and average Nusslet numbers in all cases considered. Ahmad and Badr [13] studied theoretically mixed convection from an elliptic tube placed in a fluctuating free stream. It is found that the heat transfer enhancement due to free-stream fluctuations is more pronounced for high Reynolds numbers and moderate Grashof numbers. Khan el al. [14] carried out an experimental investigation to study forced convection cross flow heat transfer of hot air over an array of elliptical tubes carrying cold water. The array consisting of 18 elliptical tubes each 30 cm long, with minor to major outside axis ratio of 0.30, and was oriented at zero angle of attack. The results showed that the Nusselt number and hence, the heat

transfer rate, increased with the increase of both air and water Reynolds numbers.

The purpose of the present study is to investigate the heat transfer characteristics and the flow behaviors around an elliptic cylinder (downstream cylinder) from two elliptic cylinders in-line arrangement. As a first step, heat transfer and flow around a single elliptic cylinder in cross flow were conducted. The present elliptic cylinders have an axis ratio 1:2, with zero angle of attack to the upstream uniform flow. Also, the effects of Reynolds number and the cylinder spacing ratio were examined.

II. EXPERIMENTAL SETUP, MEASURING INSTRUMENTS AND ROCEDURE

The experimental setup consists mainly of a suction wind tunnel of cross section 200 × 200 mm and length of 2000 mm, where air is supplied to the test section through a bellmouth intake. The main components of the test rig are: a centrifugal blower, air passage, test section, and measuring instruments as shown in figure (1). The air-flow discharge is controlled at the outlet of the air blower by means of a variable area outlet gate. Various values of Reynolds number based on tube major axis length were utilized in the experiments which ranged from 3,450 to 45,420.

For heat transfer measurements, an elliptic cylinder is heated electrically at a constant heat flux as shown in details in figure (2). The tested elliptic cylinder is made of wood with a length of 200 mm and a major axis length of 30 mm with an axis ratio of 1:2. A nickel-chorme tape of 0.2 mm thickness and 5 mm width is wound helically over the outer surface of the wooden cylinder with a pitch of 1 mm to attain a uniform heat flux. Twenty one copper-constantan thermocouples (0.4 mm diameter) were distributed circumferentially, embedded on the cylinder surface, and fixed at the back of the nickel-chrome heater tape to measure the surface temperature of the heated cylinder. To confirm a uniform temperature distribution, three thermocouples are installed at the two ends and at mid span of the tested cylinder to measure the axial temperature. Two thermocouples were used to measure air temperature entering and leaving the test section. One similar elliptic cylinder was placed at in-line arrangement upstream the tested cylinder at different cylinder spacing ratios (S_x/c) of 1.5, 2.5, and 4.0. The cylinder spacing , is defined as the streamwise distance between two centers of the cylinders. The line through the centers of the elliptic cylinders is aligned with the flow direction and their angle of attack is zero (major axis is horizontal). The arrangement of the two elliptic cylinders is schematically represented in figure (3). Flow measurements are carried out using unheated elliptic cylinder which is used for static pressure measurements in a suction-type wind tunnel. The test section has a dimension of 200 mm wide, 200 mm height, and 2000 mm length. The elliptic cylinder is made of a PVC and has an axis ratio of 1:2 and is mounted at the mid-span of the test section. The static pressure distributions around the cylinder were measured by means of seventeenth pressure holes (0.5 mm diameter) which were arranged spirally on the outer surface. The static pressure coefficient C_p is calculated from equation :

$$C_p = \left(P_\infty - P_{st}\right)/0.5\rho U_o^2 \quad (1)$$

A data acquisition system is connected to the pressure holes to measure the static pressure distributions. This system is capable of recording and processing data from up to 100 measuring points and take the average of 100 readings for each point. The system consists of solenoid valves, a pressure transducer, data acquisition card, and a PC (Pentium type). The accuracy of the measuring system was about ±1%. The local heat transfer coefficient and the corresponding Nusselt

number are calculated, respectively, as follows:

$$h = \frac{q_w}{(T - T_{bx})} \quad (2)$$

$$Nu = (hc/k) \quad (3)$$

III.COMPUTATIONAL TECHNIQUE

The flow and thermal computations for forced convection around two elliptic cylinders in-line arrangement are carried out by using CFD (ANSYS) code. Heat exchangers consist of circular tubes which are arranged in rows. The turbulence two-dimensional model for the flow and thermal fields is used where the computation advantages could be obvious [15]. This assumption is valid because the cylinder spacing between elliptic tubes in each row is small compared to the spacing between the rows and the length of each row is higher than the elliptic tube major axis. All solutions apply a parabolic flow profile at inlet and zero velocities along the walls. Forced air cooling through a channel is used for heat dissipation from elliptic tubes with different spacing distances. The two-dimensional governing equations for incompressible flow in non-dimensional form are given as:-

Continuity equation:

$$\frac{\partial u}{\partial x} + \frac{\partial v}{\partial y} = 0 \quad (4)$$

Momentum equation:

$$u\frac{\partial u}{\partial x} + v\frac{\partial u}{\partial y} = \frac{1}{Re}\left(\frac{\partial^2 u}{\partial x^2} + \frac{\partial^2 u}{\partial y^2}\right) - \frac{\partial p}{\partial x} \quad (5)$$

Energy equation

$$u\frac{\partial \theta}{\partial x} + v\frac{\partial \theta}{\partial y} = \frac{1}{Re.Pr}\left(\frac{\partial^2 \theta}{\partial x^2} + \frac{\partial^2 \theta}{\partial y^2}\right) \quad (6)$$

where $x = X/c$, $u = U/U_o$, $p = P/(\rho U_o^2)$, and $\theta = [(T - T_o)k]/(q_w h_m)$, q_w is the heat flux, T_o and U_o are the temperature and velocity of the air flow, respectively. In the present work, the flow velocity at all solid surfaces is zero and a fully developed parabolic flow enters the domain. The pressure set to zero at the channel exit while the axial velocity component is calculated to satisfy the velocity mass conservation. Constant heat flux is applied to the surfaces of each elliptic tube and a uniform inlet air temperature is applied at duct inlet. The upper and lower duct walls are insulated thermally $d\theta/dy\big|_{y=0,y=H} = 0$. The program utilizes the finite element approach which uses quadratic elements. Fine elements were created nearest to the elliptic cylinders. The present work presents the predicted temperatures of elliptic tube surface in a forced convection system by performing the CFD analysis.

IV.EXPERIMENTAL RESULTS AND DISCUSSION

The present experimental work is used to gain a better understanding of the heat transfer characteristics and the flow behaviors around a single elliptic cylinder in cross flow and also around two elliptic cylinders in-line arrangement.

IV.1 Flow Results

Figure (4) shows the local static pressure coefficient distributions versus the circumferential path distance ratio (s/c) around downstream elliptic cylinder for different cylinder spacing ratios (S_x/c) and compared with a single cylinder ($S_x/c=\infty$) for Re = 8,000 . The maximum static pressure occurs at stagnation point (s/c=0) and decreases rapidly with increasing surface path distance upward and downward the stagnation point until it reaches to a minimum value at about (s/c=±0.2), and downstream this position, the pressure begins slowly to increase. The flow around cylinder starts to separate in cylinder front part at s/c=±0.65 and reaches nearly a constant value between s/c=±0.8 and s/c=±1.4. Figure (5) illustrates the effect of Reynolds number on the average static pressure coefficient for different values of cylinder spacing ratio. The static pressure decreases as the Reynolds

number increases for different values of (S_x/c) within 8,000≤Re≤15,000. It is observed that the static pressure at S_x/c=2.5 has the lowest values than those at S_x/c=1.5 and S_x/c =4.0. This occurs because a higher flow distortion and acceleration are found between the two cascaded cylinders. As the spacing ratio (S_x/c) increases to 4.0, the static pressure increases and reaches nearly the values of average static pressure for a single cylinder (in absence of the upstream cylinder). Therefore, the optimum heat transfer enhancement may be attained at cylinder spacing ratio of 2.5 when Reynolds number less than 15,000.

IV.2 Heat Transfer Results

IV.2.1 Single elliptic cylinder

Experiments were carried out for a single elliptic cylinder at constant heat flux conditions, zero angle of attack, and Reynolds number ranged from 3,450 to 45,420. The variations of both normalized temperature ratio and local Nusselt number distributions around the whole circumference of the elliptic cylinder are plotted for different Reynolds numbers as shown in figures (6) and (7), respectively. The results show that the normalized temperature ratio, $(T-T_{bx})/T_o$, decreases monotonically as the Reynolds number increases. It is found that the local Nusselt number reaches a maximum at the upstream stagnation point (the leading edge), and steeply decreases on both sides of the cylinder with increasing the path surface distance (s/c) due to the development of the laminar boundary layer, and subsequently reaches a minimum near the separation point. The phenomenon of increasing the local Nusselt number may be attributed to the flow reattachment that occurred immediately at the leading edge region. However, the flow separates at about $S_x/c = \pm 0.65$ which is located at nearly of the minor axis of the elliptic cylinder. The separation point corresponds to the beginning of the nearly constant local Nusselt number [16]. It is clear that the symmetry of the local Nusselt number distribution on the upper and lower surfaces is satisfactory at all the Reynolds number. In the following, the positive value of (s) is located on the upper surface of the cylinder. It may be reasonable to consider that the whole tested Reynolds number range is included within the subcritical flow regions, since the heat transfer distribution shows no essential change with Reynolds number [4,17].

The average Nusselt number is calculated from present experimental data for a single elliptic cylinder with zero angle of attack and compared with the correlation proposed by Ota et al. [4], and fair agreement is found as shown in Fig. (8). It is found that the average Nusselt number increases almost linearly with Reynolds number in logarithmic scale. Also, it is noticed that the average Nusselt number for a single elliptic cylinder over the whole Reynolds number range studied is still higher than that for a circular cylinder, as compared with the correlation proposed by Churchill and Bernstein [18]. Moreover, it is observed in figure (8) that the presented results agree well with the previous data of [4], and there is a little difference between them and this may be attributed to the change in the elliptic cylinder axis ratio. Finally, the average Nusselt number for a single elliptic cylinder with zero angle of attack is correlated utilizing the present experimental data as function of Reynolds number as follows:

$$Nu_{s,m} = 0.713 Re^{0.514} \quad (7)$$

where the constants are obtained by curve fitting, based on a least squares method through the present data. The maximum deviation of the measured data from the above correlation is about 7% within the Reynolds number range of (3,450 ≤ Re ≤ 45,420). A satisfactory agreement in the above comparison has confirmed that the

experimental procedure employed is adequate and the results obtained are reliable.

IV.2.2 Two elliptic cylinders in-line arrangement

In the present work, the heat transfer and flow behavior around the downstream elliptic cylinder of two elliptic cylinders in-line arrangement are investigated experimentally and theoretically. The elliptic cylinders are arranged in-line with zero angle of attack and the longitudinal cylinder spacing ratio, (S_x/c) is ranged from 1.5 to 4.0, where S_x denotes the distance between the cylinder centers and c is the major axis length.

The variations of both the normalized local temperature ratio and the local Nusselt number versus the surface path distance ratio, for different cylinder spacing ratios (S_x/c) are shown in figures (9) – (11) and figures (12) – (14), respectively. Figures (9-14) show that both the local temperature ratio and the local Nusselt number various remarkably on the whole of the cylinder surface with the cylinder spacing ratio. At a narrow spacing ratio of S_x/c=1.5, two shear layers separate from the upstream cylinder and attach to the downstream cylinder. As shown in figure (12), the local Nusselt number attains a maximum at the attachment point. The flow inside a wake region bounded by two cylinders and two separated shear layers is stagnant and then local Nusselt number is low at the leading edge region. Downstream of the attachment point, the Nusselt number decreases with the surface path distance because of a developing boundary layer. The local Nusselt number reaches a minimum nearest to the separation point and then increases slightly in the separated flow region.

However, an increase of S_x/c from 1.5 to 2.5 brings about a great variation of the local Nusselt number distribution, especially on the upstream surface as shown in figure (13). It is found that the local Nusselt number attains a maximum value at the leading edge and decreases with the surface distance to reach a minimum value. Then, in the separated flow region, the local Nusselt number is slightly increased. The drastic variation of the local Nusselt number at the leading edge may be attributed to an occurrence of the jumping phenomenon for the wake of the upstream cylinder. That is, if the spacing between two cylinders is large enough, the separated shear layers from the upstream cylinder roll up upstream of the downstream cylinder and the main flow at free stream temperature is entrained onto the upstream surface of the downstream cylinder [6,19]. This results in a higher heat transfer rate there. Figure (14) shows the local Nusselt number distribution at greater spacing ratio of S_x/c=4.0. It is clear that the local Nusselt number distribution becomes similar to that for the single cylinder, where the values of local Nusselt number are generally higher on the downstream cylinder than on the single cylinder because of the highly turbulent flow.

Figure (15) shows the variation of the average Nusselt number with Reynolds number at different spacing ratios. It is observed that the average Nusselt number increases as the Reynolds number increases at all the cylinder spacing ratios examined. Generally the results indicated that, at Reynolds number lower than about 12,000 the average Nusselt number is higher at each of S_x/c = 2.5 and 4.0. However, at Reynolds number higher than 16,000, the average Nusselt number is higher at lower value of spacing ratio, S_x/C = 1.5. The maximum enhancement ratio of the average Nusselt number (average Nusselt number for downstream cylinder/average Nusselt number for single elliptic cylinder) is found to be approximately 1.72 and 1.68 at Sx/c=1.5 and and 2.5 when Re = 8,200 and 45,420, respectively, as shown in figure (16).

Furthermore, the present experimental data for the downstream cylinder with different spacing ratios are used to correlate the average Nusselt number as a function of the Reynolds number (Re) and spacing ratio (S_x/c), as follows:

$$Nu_m = 1.53(Re)^{0.49}(S_x/c)^{-0.1} \quad (8)$$

where this correlation, equation (8) is valid within ±10% maximum deviation with the present experimental data for the ranges of Reynolds number ($3{,}450 \le Re \le 45{,}420$), and spacing ratio ($1.5 \le (S_x/c) \le 4.0$).

Figure (17) represents a comparison between the results of average Nusselt number versus the cylinder spacing ratio (S_x/c) that was obtained with different values of Re to that was obtained by Ota, et al. [6] for two elliptic cylinder in-line arrangement.

V. COMPUTATIONAL AND FLOW VISUALIZATION RESULTS

The effect of cylinder spacing ratio (S_x/c) on the flow and heat transfer characteristics (velocity contours and vectors, flow pattern, and temperature field) is illustrated in figures (18) and (19) at Re =21,288. Four values of cylinder spacing ratio have been studied of 1.5, 2.5, 4.0 and ∞ (case of single elliptic cylinder), and the air flow direction from left to right. Two values of spacing ratio were investigated in figure (18), namely of S_x/c=1.5 and 2.5. The downstream cylinder has a lower dimensionless temperature at S_x/c =1.5 than that for S_x/c=2.5, due to the higher velocity values with a greater air cooling rate. For small spacing ratio S_x/c =1.5, air flow movements and activity is observed in the enclosed space between the cylinders. Flow visualization by means of a high speed digital Camera was performed in a smoke tunnel to complete the view picture of the phenomenon. The visualization tests were carried out for channels with elliptic cylinders at different values of spacing ratio (S_x/c=1.5, 2.5, 4.0, and ∞). It is observed that as the spacing distance ratio increases the recirculating zone formed upstream the test elliptic cylinder extended slightly and a horseshoe vortex is formed in front of the first cylinder. At small spacing ratio S_x/c =1.5, it is observed that the flow in the space between the two cylinders becomes more unsteady with rotational vortices and some exchange of flow with the main free stream occurs. For S_x/c =4.0, the downstream cylinder has a higher temperature than that for S_x/c =2.5 and S_x/c =1.5 where the recirculation region no longer exists between the two cylinders and the flow pattern is similar to that of single cylinder which has the highest temperature. At small spacing ratio S_x/c =1.5, the boundary layer separates from the two sides of the upstream elliptic cylinder produces vortices that are impingement the downstream cylinder at about s/c ≈0.25. At high spacing ratio, the separated shear layers are intersecting upstream the downstream cylinder.

VI. CONCLUSIONS

In the present work an experimental and theoretical investigation of the heat transfer characteristics and flow behavior around each of a single elliptic cylinder and the downstream cylinder from of two elliptic cylinders in line arrangement. The elliptic cylinder examined having an axis ratio of 1:2. The effects of Reynolds number (based on major axis length) and the cylinder spacing ratio (S_x/c) are examined. Experiments are carried within Reynolds number ranged from 3,450 to 45,420 at zero angle of attack. The main conclusions are summarized as follows:

1- For a single elliptic cylinder, the local Nusselt number reaches a maximum at the upstream stagnation point (the leading edge), and steeply decreases on both sides of the cylinder with increasing the surface distance and subsequently reaches a minimum near the separation point.

2- The flow is separated from the single elliptic cylinder at about $S_x/c = \pm 0.65$ which is located at nearly minor axis of the elliptic cylinder.
3- The average Nusselt number for a single elliptic over the whole Reynolds number range studied is still higher than that for the circular cylinder.
4- For two elliptic cylinders (in line arrangement), the flow around the downstream cylinder exhibits a very complicated variation with spacing ratio (S_x/c). At small spacing ratio ($S_x/c = 1.5$), the separated shear layers from upstream cylinder attach on to the downstream cylinder and the flow between two cylinders is relatively slow moving. At large spacing ratio ($S_x/c \geq 2.5$), the two shear layers roll up in front of the downstream cylinder, and the main flow at free stream temperature is entrained onto the upstream surface of the downstream cylinder.
5- For the examined spacing ratio ranged from 1.5 to 4.0, the average Nusselt number of the downstream cylinder is still much higher than that of the single elliptic cylinder.
6- At Reynolds number lower than about 12,000 the average Nusselt number is higher at each of $S_x/c = 2.5$ and 4.0. However, at Reynolds number higher than 16,000, the average Nusselt number is higher at lower value of spacing ratio, $S_x/c = 1.5$.
7- The maximum enhancement ratio of the average Nusselt number (average Nu for downstream cylinder/average Nu for single elliptic cylinder) is found to be approximately 1.72 at $S_x/c = 4.0$ and Re=8,200 (or at $S_x/c = 1.5$ and Re=45,420).
8- Empirical correlation of the average Nusselt number for both the single elliptic cylinder and the downstream cylinder from two cylinders in line arrangement are obtained as function of Reynolds number and cylinder spacing ratio.

NOMENCLUTURE

b = minor axis length of elliptic cylinder, m
c = major axis length of elliptic cylinder, m
C_p= static pressure coefficient, $C_p = (P_\infty - P_{st}) / 0.5\rho U_o^2$
Cp_m = average static pressure coefficient
h_m = average heat transfer coefficient to air stream, $W/m^2.{}^oC$
H = duct height, m
k = fluid thermal conductivity, $W/m.{}^oC$
Nu = local Nusselt number.
Nu_m = average Nusselt number around the elliptic cylinder.
$Nu_{s,m}$ = average Nusselt number around a single elliptic cylinder.
P = pressure, N/m^2
P_∞ = ambient static pressure , N/m^2
P_{st}=local static pressure distributions at span wise mid-plane around elliptic cylinder, N/m^2
p = non-dimensional pressure $= P/(\rho U_o^2)$.
q_w = net heat flux, W/m^2.
Re = Reynolds number = $U_o\, c/\nu$.
s = surface distance from the leading edge, taken as positive along the upper side, m
S_x= cylinder spacing distance, (distance between two cylinder centers), m
T = local surface temperature, ^oC
T_m = average surface temperature, ^oC
T_o = average inlet air temperature, ^oC
T_{bx} = local mean bulk temperature, ^oC
U = stream wise velocity component, m/s.
U_o = upstream mean velocity, m/s.
u = non-dimensional streamwise velocity component $= U/U_o$
v = non-dimensional velocity component in normal direction.
X = stream wise length of model

x = non-dimensional stream wise coordinate.
Y = normal coordinate.
y = non-dimensional normal coordinate.

Greek

α = angle of attack
θ = non-dimensional temperature.
ν = kinematics viscosity, m^2/s

Subscripts

b = bulk
o = upstream flow.
st = static
s = single cylinder
w = wall
x = local distance in the axial direction

REFERNCES

[1] Kreith, F., Principles of heat transfer, Third edition, Harper&Row publ., 1976.

[2] Ruth, E. K., "Experiments on a cross flow heat exchanger with tubes of lenticular shape," Trans. ASME, Journal Heat Transfer, Vol. 105, No. 3, pp. 571-577, 1983.

[3] Nishiyama, H., Ota, T., and Matsuno, T., "Forced convective heat transfer from two elliptic cylinders (tandem arrangement in opposite directions)," Trans. Jpn. Soc. Mech. Eng. Vol. 52, No. 479, ser. B, pp. 2677-2681, 1986.

[4] Ota, T., Nishiyama, H., and Taoka, Y., "Heat transfer and flow around an elliptic cylinder," Int. J. Heat Mass Transfer, Vol. 27, No. 10, pp. 1771-1779, 1984.

[5] Ota, T., and Nishiyama, H., "Flow around two elliptic cylinders in tandem arrangement," Transactions of the ASME, Journal of Fluids Engineering, Vol. 108, pp. 98-103, March 1986.

[6] Ota, T., Nishiyama, H., Kominami, J., and Sato, K., "Heat transfer from two elliptic cylinders in tandem arrangement," Transaction of the ASME, Journal of Heat Transfer, Vol. 108, pp. 525-531, august 1986.

[7] Ota, T., Nishiyama, H., and Taoka, Y., "Flow around an elliptic cylinder in the critical Reynolds number regime," Trans. ASME, Journal of Fluids Engineering, Vol. 109, pp. 149-155, June 1987.

[8] Nishiyama, H., Ota, T., and Matsumo, T., "Heat transfer and flow around elliptic cylinders in tandem arrangement," JSME, International Journal, series II, Vol. 31, No. 3, pp. 410-419, 1988.

[9] Badr, H. M., and Shamsher, K., "Free convection from an elliptic cylinder with major axis vertical," Int. J. Heat Mass Transfer, Vol. 36, No. 14, pp. 3593-3602, 1993.

[10] Kondjoyan, A., and Daudin, J. D., "Effects of free stream turbulence intensity on heat and mass transfers at the surface of a circular cylinder and an elliptical cylinder, axis ratio 1:4," Int. J. Heat Mass Transfer, Vol. 38, No. 10, pp. 1735-1749, 1995.

[11] Chew, Y. T., Luo, S. C., and Guo, T., "Numerical simulation of incompressible viscous flow around an elliptic cylinder", Proceedings of International Congress on Fluid Dynamics and Propulsion, Cairo, Egypt, pp. 296-303, December 29-31, 1996.

[12] Badr, H. M., "Laminar natural convection from an elliptic tube with different orientations," Trans. ASME, Journal of Heat Transfer, Vol. 119, pp. 709-718, November 1987.

[13] Ahmad, E. H., and Badr, H. M., "Mixed convection from an elliptic tube placed in a fluctuating free stream," International Journal of Eng. Science, Vol. 39, pp. 669-693, 2001.

[14] Khan, M. G., Fartaj, A., and Ting, D. S.-K., "An experimental characterization of cross-flow cooling of air via an in-line elliptical tube array," International Journal of Heat and Fluid Flow, pp. 1-12, 2004.

[15] ANSYS, "CFD FLOTRAN Analysis Guide," ANSYS, Inc., 2001.

[16] Mahmoud, M. H., Abdalla, S. H., Saad A. E., Experimental investigation of fluid flow and heat transfer around circular cylinder-flat and curved plates combinations. Ph.D. Thesis, Faculty of Engineering, Cairo University, Egypt, 1998.

[17] Drake, R. M., Seban, R. A., Doughty, D. L., and Levy, S., "Local heat-transfer coefficients on surface of an elliptic cylinder, axis ratio 1:3, in a high-speed air stream," Trans. of ASME, Vol. 75, pp. 1291-1302, 1953.

[18] Churchill, S. W., and Bernstein, M., "A correlating equation for forced convection from gases and liquids to a circular cylinder in cross-flow," ASME Journal of Heat Transfer, Vol. 99, pp. 300-305, 1977.

[19] Zdravkovich, M. M., "Review of flow interference between two circular cylinders in various arrangements", ASME Journal of Fluids Engineering, Vol. 99, pp. 618-633, 1977.

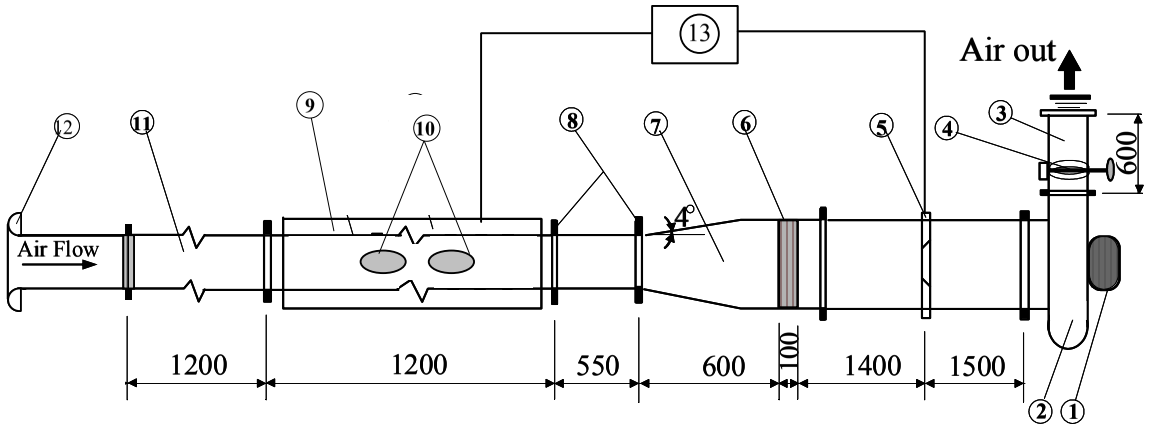

1. A.C electric motor.8. Flanges.
2. Air blower.9. Test section.
3. Exit duct.10. Elliptic cylinders.
4. Air gate controller.11. Main duct.
5. Flow orifice meter.12. Bell-mouth intake.
6. Straightener. 13. Micro-manometer.
7. Transformation duct.

Fig.(1): Schematic diagram of the test rig.

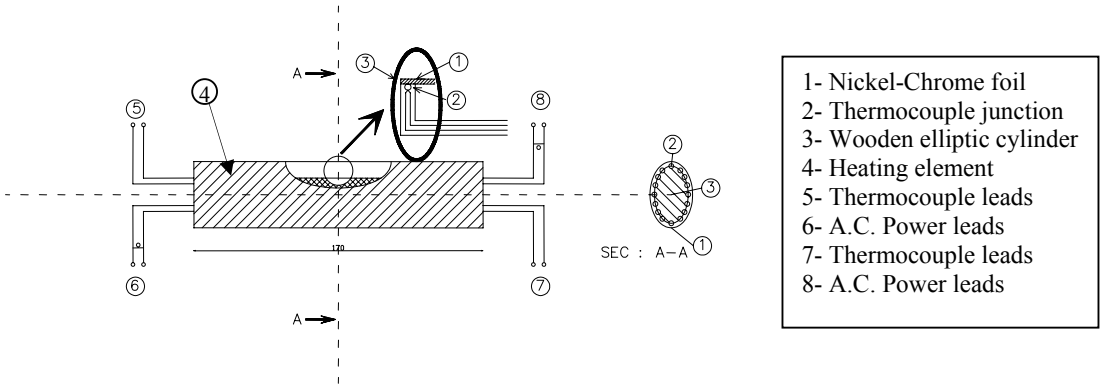

Fig. (2): Construction of heating elliptic cylinder.

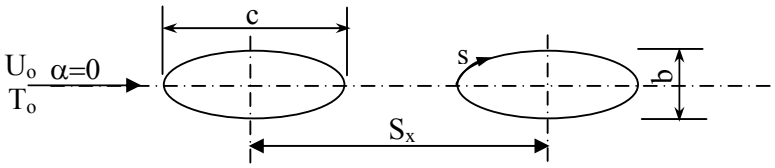

Fig. (3): Arrangement of two elliptic cylinders and coordinates system

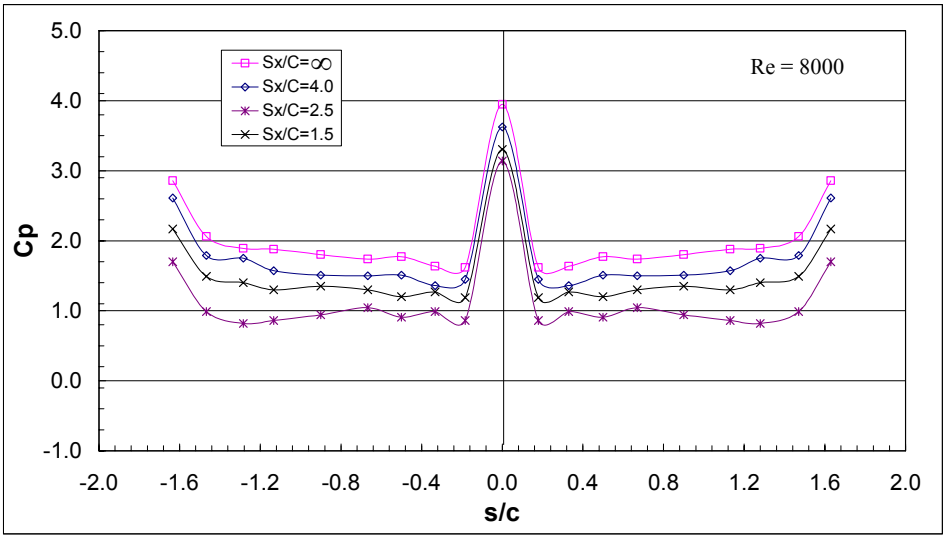

Fig. (4): Variation of local static pressure coefficient around downstream elliptic cylinder for different values of spacing cylinder ratio and (Re = 8000)

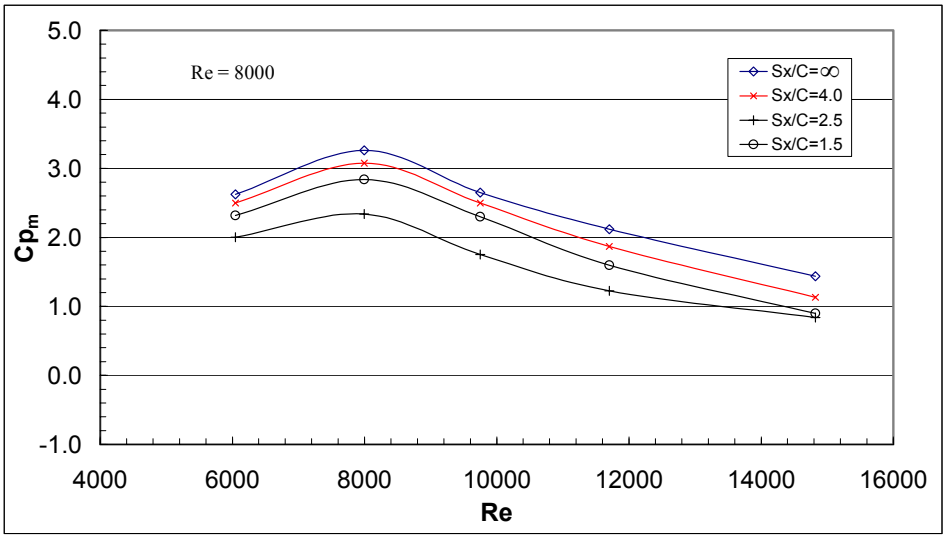

Fig. (5): Variation of average static pressure coefficient around downstream elliptic cylinder for different values of spacing cylinder ratio and (Re = 8000)

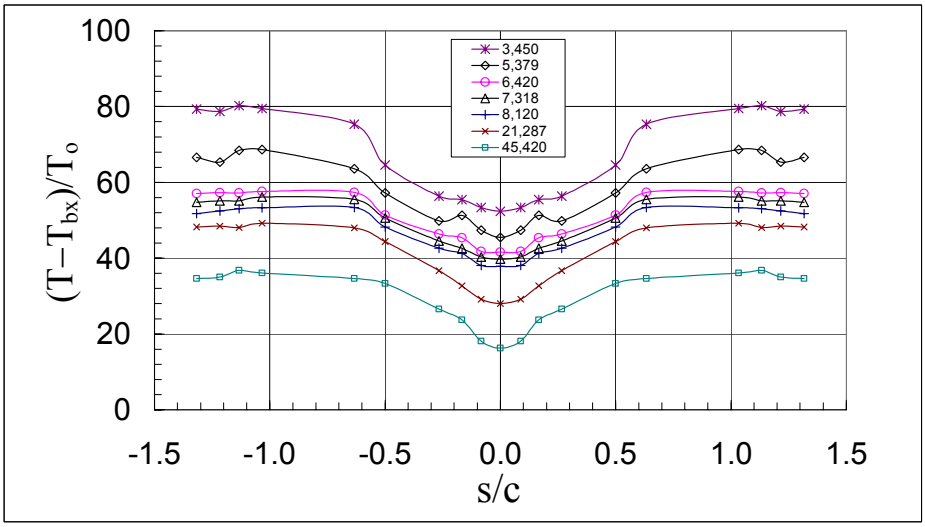

Fig. (6): Variation of normalized local temperature ratio versus s/c for a single elliptic cylinder at different Re.

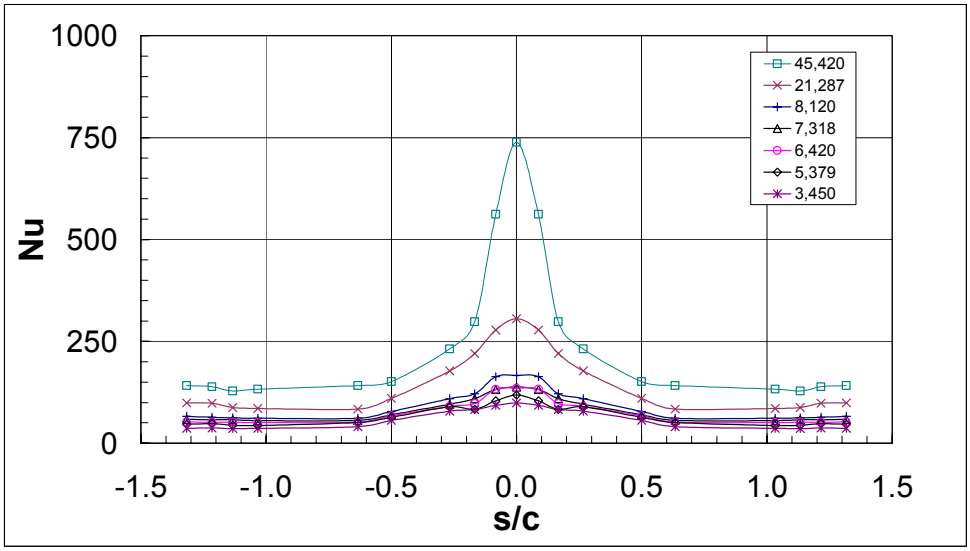

Fig. (7): Variation of local Nusselt number versus s/c for a single elliptic cylinder at different Re.

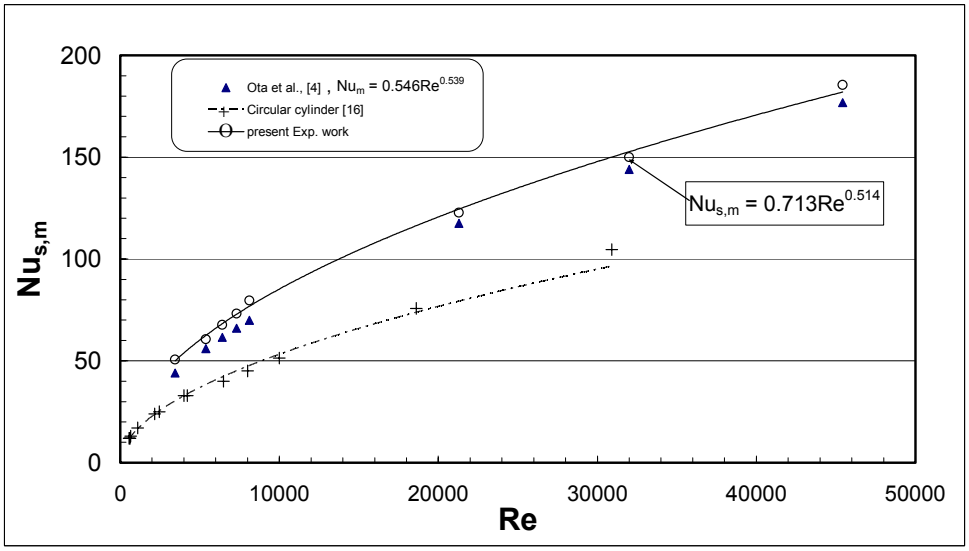

Fig.(8): Comparison of present results for average Nusselt number with previously published results, (single elliptic cylinder only)

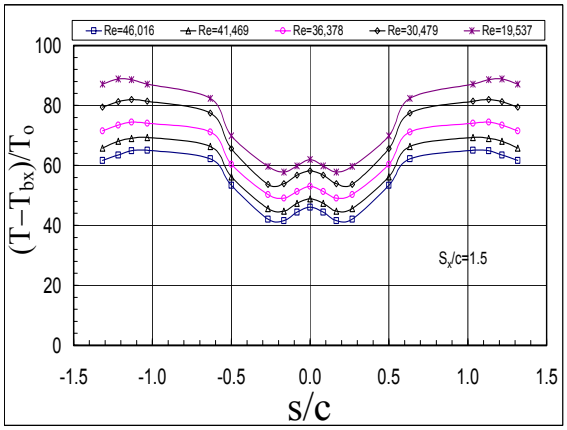

Fig. (9): Variation of normalized local temperature ratio versus s/c for downstream elliptic cylinder at $S_x/c=1.5$

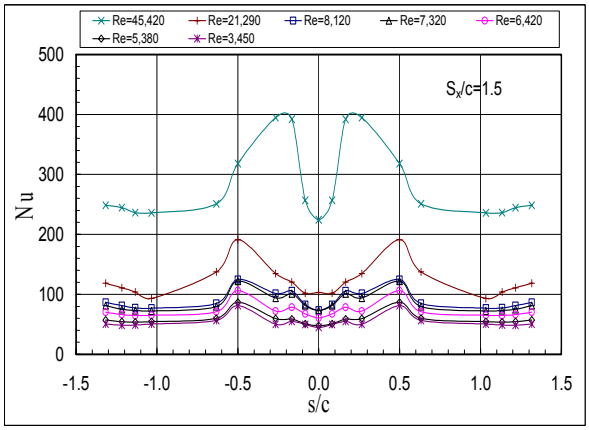

Fig. (12): Variation of normalized local Nusselt number versus s/c for downstream elliptic cylinder at $S_x/c=1.5$

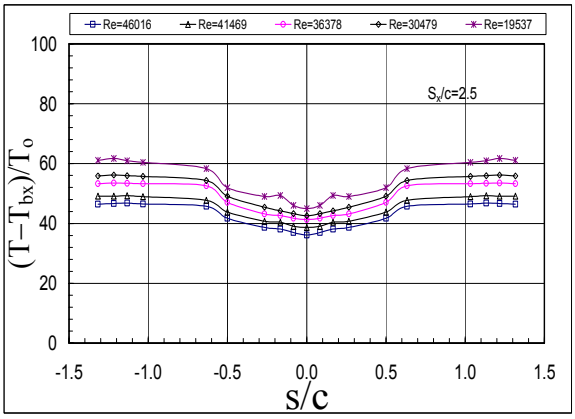

Fig. (10): Variation of normalized local temperature ratio versus s/c for downstream elliptic cylinder at $S_x/c=2.5$

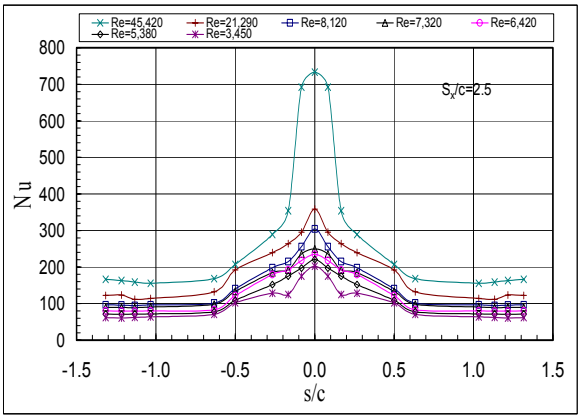

Fig. (13): Variation of normalized local Nusselt number versus s/c for downstream elliptic cylinder at $S_x/c=2.5$

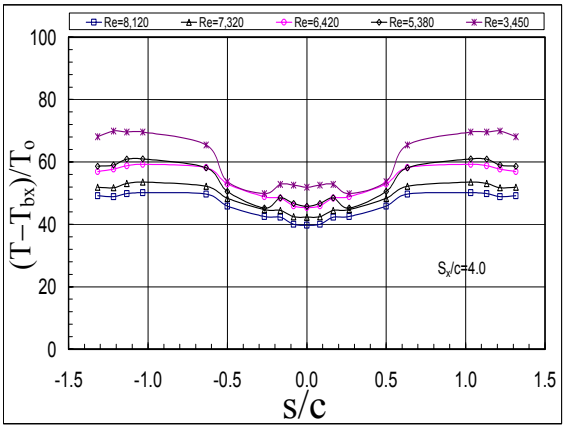

Fig. (11): Variation of normalized local temperature ratio versus s/c for downstream elliptic cylinder at $S_x/c = 4.0$

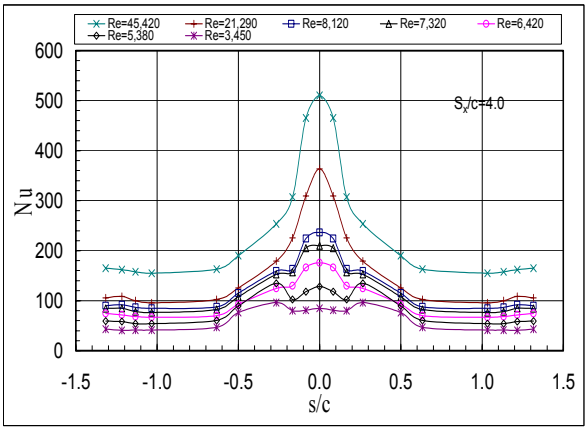

Fig. (14): Variation of normalized local Nusselt number versus s/c for downstream elliptic cylinder at $S_x/c=4.0$

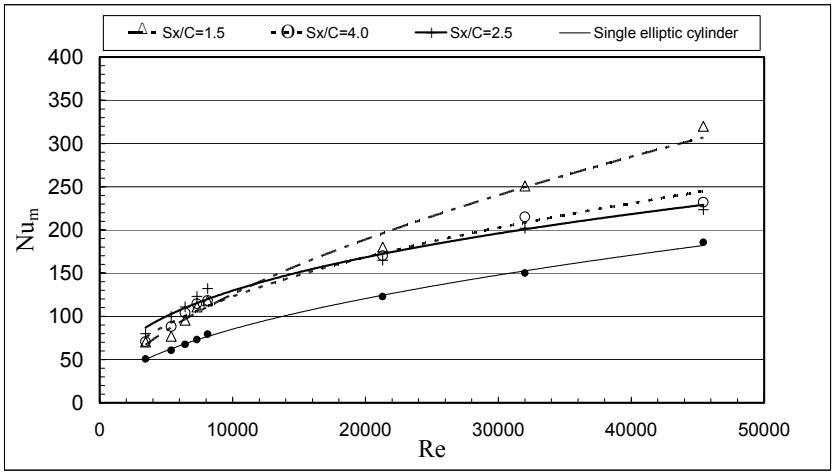

Fig.(15): Variation of the average Nusselt number enhancement ratio versus Reynolds number at different cylinder spacing ratios (S_x/c).

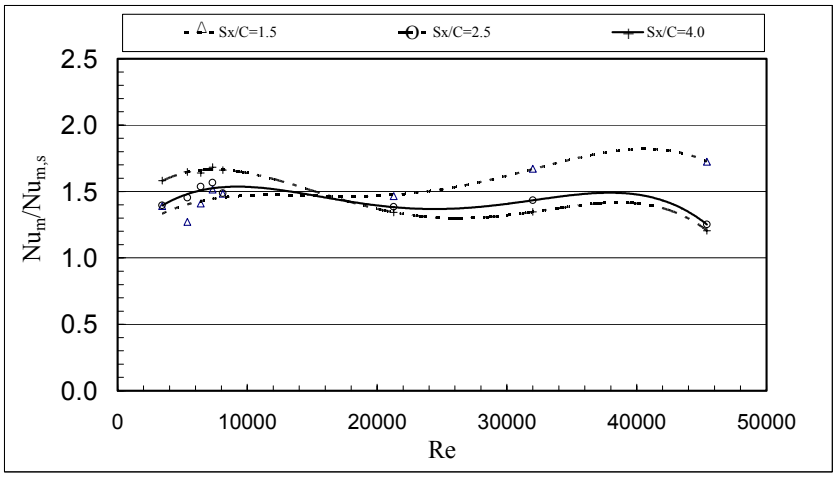

Fig.(16): Variation of average Nusselt number ratio with Reynolds number for different values of cylinder spacing ratio, S_x/c.

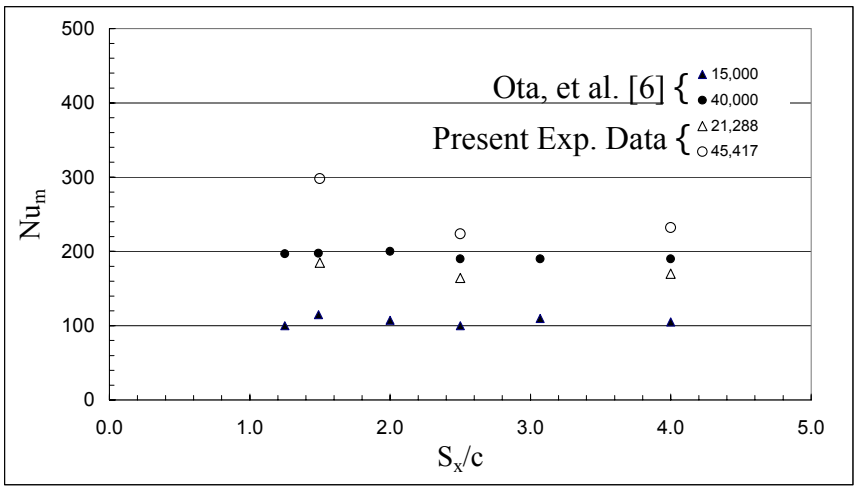

Fig.(17): Comparison between the experimental results for different values of cylinder spacing ratio (c/S_x) and Reynolds number with that of Ota et al. [6].

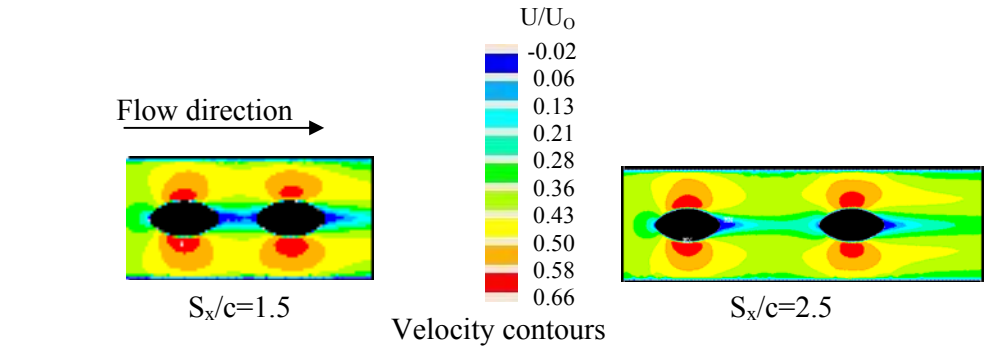

Velocity contours

Velocity vectors

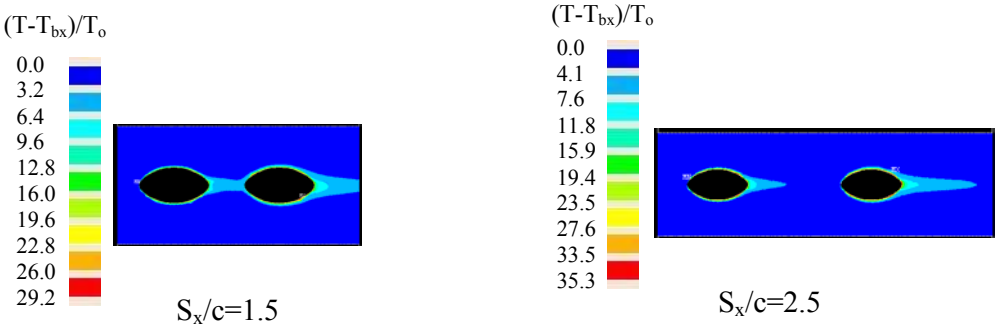

Temperature contours

Flow visualization

Fig. (18): Velocity contours, vectors, normalized temperature contours, and flow visualization around elliptic tubes in-line arrangement with different cylinder spacing ratios and (Re = 21,288)

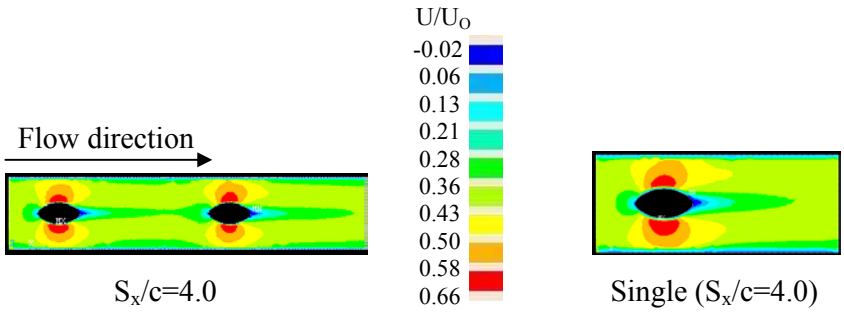

Velocity contours

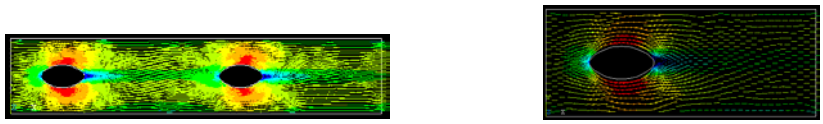

Velocity vectors

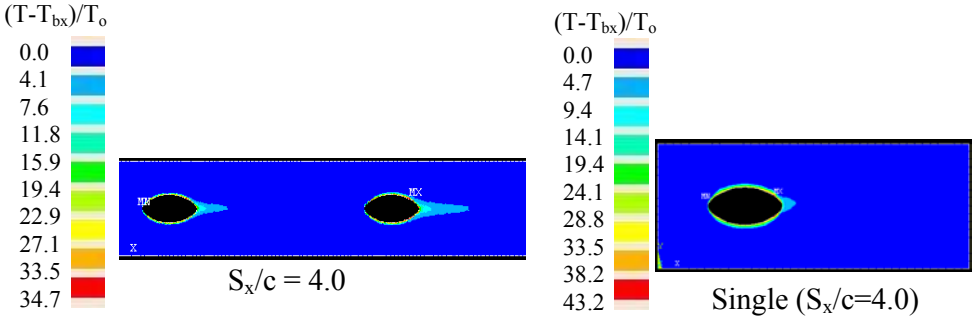

Temperature contours

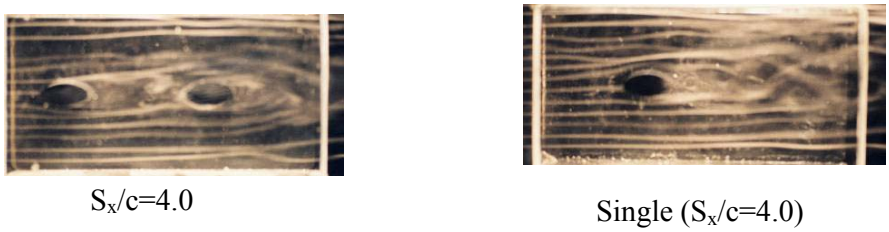

Flow visualization

Fig. (19): Velocity contours, vectors, normalized temperature contours, and flow visualization around elliptic tubes in-line arrangement with different spacing ratios at (Re = 21,288)